A single receptor encoded by *vzg-1*/*lp*$_{A1}$/*edg-2* couples to G proteins and mediates multiple cellular responses to lysophosphatidic acid

NOBUYUKI FUKUSHIMA*, YUKA KIMURA*†, AND JEROLD CHUN*†‡§

*Department of Pharmacology, †Neurosciences Program, and ‡Biomedical Sciences Program, School of Medicine, University of California at San Diego, La Jolla, CA 92093-0636

ABSTRACT Extracellular lysophosphatidic acid (LPA) produces diverse cellular responses in many cell types. Recent reports of several molecularly distinct G protein-coupled receptors have raised the possibility that the responses to LPA stimulation could be mediated by the combination of several uni-functional receptors. To address this issue, we analyzed one receptor encoded by *ventricular zone gene-1* (*vzg-1*) (also referred to as *lp*$_{A1}$/*edg-2*) by using heterologous expression in a neuronal and nonneuronal cell line. VZG-1 expression was necessary and sufficient in mediating multiple effects of LPA: [^{3}H]-LPA binding, G protein activation, stress fiber formation, neurite retraction, serum response element activation, and increased DNA synthesis. These results demonstrate that a single receptor, encoded by *vzg-1*, can activate multiple LPA-dependent responses in cells from distinct tissue lineages.

Lysophosphatidic acid (LPA) is a simple phospholipid, and extracellular LPA has been shown to activate second messenger pathways to elicit diverse cellular responses in many types of cells (1–7). Although nonreceptor mechanisms resulting from its perturbation of the cell membrane may contribute, LPA appears to exert its major effects through a specific cell surface receptor coupled to guanine nucleotide regulatory (G) proteins that activate pertussis toxin (PTX)-sensitive and -insensitive pathways. The PTX-sensitive pathway uses G_i and inhibits adenylyl cyclase (1). In addition, transcriptional activation of immediate-early genes, subsequent DNA synthesis, and cell proliferation appear to be mediated by activation of the G_i-p21^{ras}–mitogen-activated protein kinase pathway (5, 7–10). LPA also stimulates a PTX-insensitive pathway resulting in actin rearrangement and stress fiber formation in fibroblast cells. This effect is known to be mediated by the small GTPase Rho, which is thought to function downstream of G protein stimulation (2, 6). This pathway also has been reported for LPA-induced neurite retraction associated with actin rearrangement in neuronal cell lines (11). Rho has been implicated further in cell cycle progression (12) and may also affect cell proliferation through activation of serum response elements (SREs) (4).

Recent studies have identified genes for at least two divergent, functional, G protein-coupled LPA receptors from mammals (13) or frogs (14); it is probable that other related but distinct receptors also exist (T. Hla, personal communication). This probability raises the formal possibility that the diverse effects produced by LPA could be accounted for by a combination of nonreceptor mechanisms with multiple, uni-functional receptors on a single cell, rather than a single, multifunctional receptor. Here, we analyze the function of *ventricular zone gene-1* (*vzg-1*) (also referred to as *lp*$_{A1}$/*edg-2*), which encodes a mammalian G

protein-coupled LPA receptor (13), in mediating LPA-dependent responses by using a heterologous expression system consisting of two cell lines from either a neuronal or nonneuronal lineage that neither expresses *vzg-1* nor responds to LPA.

EXPERIMENTAL PROCEDURES

Lipids, Vectors, and C3 Exoenzyme. Oleoyl-LPA, lysophosphatidic choline, lysophosphatidic ethanolamine, lysophosphatidic glycerol, and phosphatidic acid were purchased from Avanti Polar Lipids (Alabaster, AL). Expression vectors used in this study are summarized in Table 1. C3 exoenzyme was expressed in *Escherichia coli* as recombinant protein (his-C3 exoenzyme) tagged with hexahistidine at the N terminus and purified by using Nickel–agarose (Qiagen) and CM-Sepharose CL-6B (Sigma) up to 95% homogeneity on SDS/PAGE, and its function was confirmed by the [^{32}P]-ADP ribosylation assay (11, 15).

Cell Culture, Transfection, [^{35}S]-Methionine/Cysteine Labeling, and Immunoprecipitation. RH7777 and B103 cells were maintained in DMEM (GIBCO/BRL) containing 10% fetal calf serum. Transient transfection used a DNA/lipofectoamine (GIBCO/BRL) complex (15 h) grown in fresh serum-free DMEM (30 h) and then assayed. Stable transfection of B103 cells used co-transfection with control or experimental vector and pSV-neo for selection by calcium phosphate (13). Stable cell lines were serum-starved for 24 h before assay (summarized in Table 1).

For detection of VZG-1 exogenously expressed, RH7777 cells were labeled with 50 μCi/ml of [^{35}S]-methionine/cysteine (1,175 Ci/mmol, NEN) in methionine/cysteine-free DMEM for 6 h. The cells were lysed with 50 mM Tris·HCl (pH 7.5), 150 mM NaCl, 5 mM EDTA, 1% (wt/vol) Triton X-100, 0.5% deoxycholate-Na, and protease inhibitor mixture (Calbiochem), immunoprecipitated with anti-flag M2 antibody (Kodak), followed by protein G-agarose chromatography, and analyzed by SDS/PAGE and then fluorography by using Amplify (Amersham). In some experiments, cells were treated with 200 ng/ml PTX (Sigma) for 18 h or 30 μg/ml his-C3 exoenzyme for 24 h in serum-free medium before membrane preparation or LPA application to cells. In the bromodeoxyuridine (BrdU) incorporation assay, toxin was re-added to cultures when LPA was applied.

Membrane Preparation, [^{3}H]-LPA Binding Assay, and [^{35}S]-GTPγS Binding Assay. Cells were harvested, homogenized in ice-cold LPA-binding buffer (20 mM Tris-HCl, pH 7.5) containing 1 mM EDTA, and centrifuged at $1,000 \times g$ for 5 min at 4°C, and the supernatant was centrifuged further at $15,000 \times g$ for 20 min at 4°C. The membrane preparation (40 μg) was incubated with 30 nM [^{3}H]-LPA (1-oleoyl-[9, 10-^{3}H]-LPA/51 Ci/mmol, NEN) in LPA-binding buffer containing 0.1% fatty acid-free BSA (Sigma) and 0.5 mM CuSO$_4$ for 2 h at 4°C, and the bound

---

Table 1.   Expression vectors and transfected cell lines used in this study

Name	Vectors
Vectors	
pflag (control)	pflag-CMV-1 (Kodak) (signal sequence followed by flag)
pflag/vzg-1 (experimental)	pflag-CMV-1 containing *vzg-1* ORF
pcDNAI (control)	pcDNAI (Invitrogen)
pcDNAI/antisense vzg-1 (control)	pcDNAI containing antisense *vzg-1*
pcDNAI/vzg-1 (experimental)	pcDNAI containing *vzg-1* ORF
pHook2 (control)	pHook2 (Invitrogen) (phOx sFv, a marker protein co-expressed)
pHook2/vzg-1 (experimental)	pHook2 containing *vzg-1* ORF
pBLCAT2*	
Stable cell lines	
E-7 (stable line for empty vector)	pcDNAI + pSV-neo
A-5 (stable line for antisense *vzg-1*)	pcDNAI/antisense vzg-1 + pSV-neo
S-3 (stable line for sense *vzg-1*)	pcDNAI/vzg-1 + pSV-neo
S-4 (stable line for sense *vzg-1*)	pcDNAI/vzg-1 + pSV-neo
S-7 (stable line for sense *vzg-1*)	pcDNAI/vzg-1 + pSV-neo
C-1 (stable line for CAT under SRE)	pBLCAT2 + pSV-neo

*From M. Karin, University of California, San Diego.

[^{3}H]-LPA was separated from free by rapid filtration through GF/C filters (Whatman) presoaked with binding buffer containing 1% normal BSA. The filters were rinsed and quantified by liquid scintillation. Nonspecific binding was determined in the presence of 5 μM unlabeled LPA. Thin-layer chromatography analysis (16) showed that [^{3}H]-LPA was not degraded during incubation (data not shown).

For [^{35}S]-GTPγS assay, membranes were prepared as above, except that TED buffer (20 mM Tris·HCl, pH 7.5/1 mM EDTA/1 mM DTT/DTT) was used for homogenization. Membranes (25 μg) were incubated in 400 μl of GTP-binding buffer (50 mM Hepes–NaOH, pH 7.5/100 mM NaCl/1 mM EDTA/5 mM MgCl$_2$/1 mM DTT) containing 0.1% fatty acid-free BSA, 0.1 nM [^{35}S]-GTPγS (1,200 Ci/mmol, NEN), and 10 μM GDP for 30 min at 30°C. The bound [^{35}S]-GTPγS was separated from free by rapid filtration through GF/C filters. The filters were rinsed and counted by liquid scintillation. Nonspecific binding was determined in the presence of 50 μM unlabeled GTPγS. [^{35}S]-GTPγS binding combined with anti-G$_{\alpha i3}$ immunoprecipitation used membranes (100 μg) incubated with 0.5 nM [^{35}S]-GTPγS as described above. To stop the reaction, 40 μl of 110 μM GTP was added, and the mixtures were centrifuged at 15,000 $\times$ *g* for 20 min at 4°C. The resulting pellet was solubilized in 50 mM Tris·HCl (pH 7.5) containing 150 mM NaCl, 5 mM MgCl$_2$, 0.6% Nonidet P-40, 1 mM EDTA, 1 mM DTT, and protease inhibitor cocktail. After centrifugation at 15,000 $\times$ *g* for 20 min at 4°C, the supernatant was incubated with anti-G$_{\alpha i3}$ antibody (recognizing G$_{\alpha i1}$ and G$_{\alpha i2}$ less than G$_{\alpha i3}$, Santa Cruz Biotechnology) for 15 h, followed by the incubation with protein G-agarose for 1 h at 4°C. Agarose beads were washed and counted by liquid scintillation.

Functional Assays. For stress fiber formation assay, RH7777 cells (3,000 cells/cm^2) were seeded on coverslips pre-coated with Cell-Tak (2 μg, Collaborative Research) and transfected. Cells were treated without or with ligand for 15 min, fixed with 4% paraformaldehyde, and permeabilized with 0.1% Triton X-100 in PBS for 30 min. Flag was visualized by anti-flag M2 antibody (0.5 μg/ml) and indirect immunofluorescence (fluorescein isothiocyanate, Vector Labs). Actin was labeled with tetramethylrhodamine isothiocyanate (TRITC)-labeled phalloidin (0.2 μg/ml, Sigma). Cells were observed by using a Zeiss fluorescence microscope. For neurite retraction assay, cells were treated without or with ligand for 30 min, fixed with 4% paraformaldehyde, and counted by using a Zeiss inverted microscope.

For chloramphenicol acetyltransferase (CAT) induction assay, clone C-1, a stable B103 cell line containing CAT under SRE control, was transfected, exposed to LPA in 0.1% fatty acid-free BSA between 40 and 48 h after transfection, and subjected to CAT ELISA (Boehringer Mannheim).
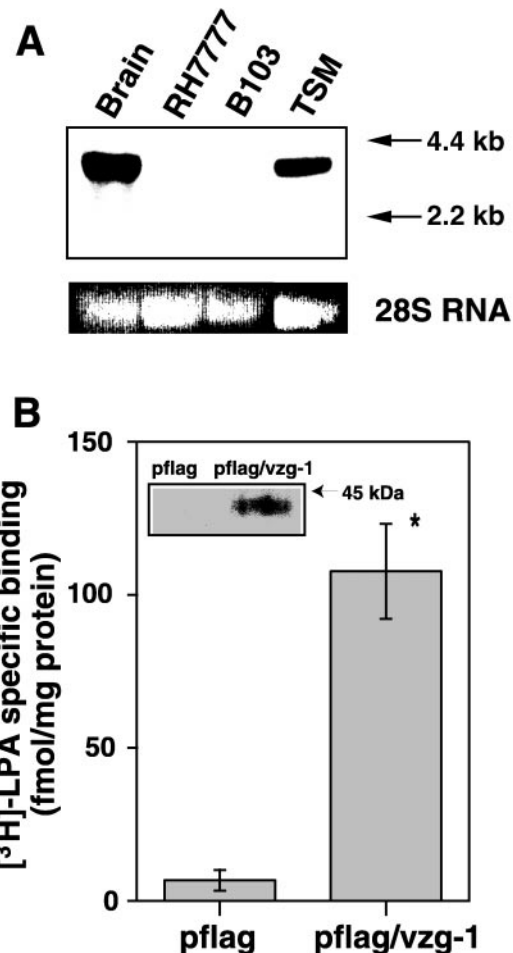

FIG. 1.   Epitope-tagged VZG-1 is expressed and functionally increases [^{3}H]-LPA binding in plasma membranes of RH7777 hepatoma expressing no *vzg-1*. (*A*) Cytoplasmic RNAs (20 μg) from RH7777 hepatoma or B103 neuroblastoma cell line serum-starved for 24 h were subjected to Northern blot analysis (24) along with *vzg-1* containing RNAs from brain and TSM, a cortical neuroblast cell line. Loading control, 28S RNA. (*B*) [^{3}H]-LPA binding in plasma membranes of RH7777 cells transiently transfected with pflag or pflag/vzg-1. Specific binding in pflag/vzg-1-transfected cells was 6.4 ± 0.9 cpm/μg protein, 60% of total binding. Data are the mean ± SEM (n = 3). ∗, $P < 0.05$ (using Student's t test) vs. pflag-transfected cells. (*Inset*) Immunoprecipitation with anti-flag antibody after [^{35}S]-methionine/cysteine labeling of pflag or pflag/vzg-1-transfected cells reveals a protein band of predicted size only in pflag/vzg-1-transfected cells.

For BrdU incorporation assay, cells were treated with LPA in 0.1% fatty acid-free BSA for 24 h, and then BrdU at 40 μM was added for the last 1 h. Cells were subjected to BrdU immunostaining (Boehringer Mannheim kit).

RESULTS

Two *vzg-1*-Null Cell Lines Are Unresponsive to LPA Stimulation. Our previous finding that there is little or no expression of *vzg-1* in liver nor neural expression outside of the embryonic cerebral cortex (13) led to identification of a hepatoma cell line, RH7777 (17), and a noncortical neuroblastoma cell line, B103 (18). Northern blot analysis (Fig. 1*A*) as well as reverse transcriptase PCR analysis (data not shown) demonstrated that these cell lines did not express *vzg-1*. In addition, these cells were not responsive to concentrations of LPA up to 1 μM, based on the multiple biochemical and morphological assays used in this study. These cell lines thus provide a heterologous expression system for the analysis of VZG-1 function.

Epitope-Tagged VZG-1 Is Expressed and Increases ^{3}H-LPA Membrane Binding. To demonstrate that a functional VZG-1, LPA receptor was being expressed, ligand binding experiments were performed by using isolated membranes from RH7777 cells transiently transfected with either pflag (control vector; see Table 1 for constructs used) or pflag/vzg-1. Only cells expressing pflag/vzg-1 showed increases in specific [^{3}H]-LPA binding (Fig. 1*B*). These observations indicated that epitope-tagged receptors were capable of specifically binding [^{3}H]-LPA.

VZG-1 Directly Couples to G_i and Probably Other G Proteins. The lipophilic nature of LPA makes it difficult to analyze ligand–receptor interactions (13, 16, 19). To overcome this problem, we also examined the functional interaction between VZG-1 and G proteins through the use of LPA-dependent labeling of G proteins by [^{35}S]-GTPγS, a hydrolysis-resistant GTP analog. The validity of this method has been demonstrated as a functional measure of G protein-coupled receptor stimulation (20–23). RH7777 cells were transfected transiently with control pflag or experimental pflag/vzg-1 and [^{35}S]-GTPγS binding assayed in isolated membranes. Basal [^{35}S]-GTPγS values of pflag-transfected cells were unaffected by LPA exposure (1 nM–1 μM; Fig. 2*A*). By contrast, basal [^{35}S]-GTPγS labeling of pflag/vzg-

1-transfected cells increased over 70% after LPA exposure in a dose-dependent manner (Fig. 2*A*).

A similar response also was observed by using [^{35}S]-GTPγS binding in membranes from B103 cell lines stably expressing *vzg-1* (Table 1; Fig. 2*B*). LPA caused no significant stimulation of [^{35}S]-GTPγS binding in controls consisting of parental cell line B103, E-7 (empty vector), or A-5 (*vzg-1* antisense). However, for both cell lines S-3 and S-7 (*vzg-1* sense) as well as TSM, a neuroblast cell line endogenously expressing *vzg-1* (13, 24), [^{35}S]-GTPγS binding increased in response to 1 nM–1 μM LPA and was blocked by pretreatment of cells with functional PTX (Fig. 2*C*). The stimulatory effects of LPA on [^{35}S]-GTPγS binding were not mimicked by structurally related compounds (Fig. 2*D*).

When [^{35}S]-GTPγS binding was combined with immunoprecipitation by using various anti-G protein antibodies including anti-$G_{\alpha i1,2}$, anti-$G_{\alpha i3}$, anti-$G_{\alpha o}$, anti-$G_{\alpha q/11}$, and anti-$G_{\alpha 13}$, only the anti-$G_{\alpha i3}$ antibody was useful for immunoprecipitation, reflecting a combination of antibody properties, expression level of endogenous G proteins, and/or the lower stoichiometry of some G proteins (e.g., G_{13}) vs. G_i for GTPγS (25, 26). LPA increased [^{35}S]-GTPγS binding in the immunoprecipitates with anti-$G_{\alpha i3}$ antibody from S-3, over A-5 (Fig. 2*E*), confirmed by Western blot of the labeled protein (data not shown), indicating that VZG-1 directly coupled to G_i. Although we could not demonstrate direct coupling of VZG-1 to other G proteins, Western blot analysis of the cell lines showed that G proteins thought to be involved in LPA signaling were expressed in control B103 and RH7777 cell lines, although the latter did not express G_o (Fig. 2*F*). These results indicated that the employed cell lines contained G proteins that have been implicated in LPA signaling and that VZG-1 directly couples to G_i.

Stress Fiber Formation Is Dependent on VZG-1 Expression and LPA Stimulation. A major effect of LPA is actin rearrangement, including stress fiber formation consisting of actin filaments (F-actin) that can be detected by fluorescently labeled phalloidin. RH7777 cells were remarkable for their lack of stress fiber formation either before or after exposure to LPA (up to 1 μM) or serum (data not shown). However, these cells did have the ability to form stress fibers when constitutively activated Rho was overexpressed in the cells (data not shown). When RH7777 cells
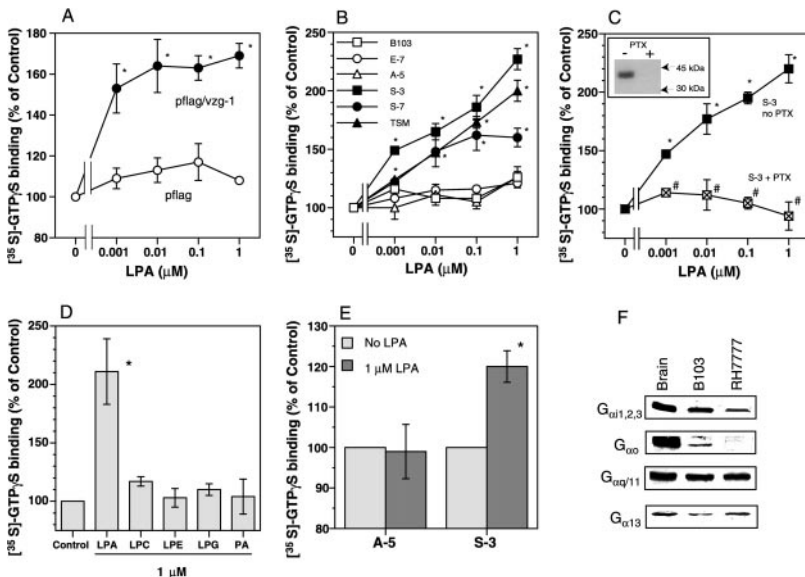

FIG. 2. VZG-1 directly couples to G_i and other G proteins in plasma membranes after LPA stimulation. (*A*) Effect of LPA on [^{35}S]-GTPγS binding to membranes from RH7777 cells transiently transfected with pflag or pflag/vzg-1. Basal [^{35}S]-GTPγS binding (no LPA) was 64.8 $\pm$ 5.3 (pflag) and 100.7 $\pm$ 6.8 (pflag/vzg-1) cpm/μg protein. Data are expressed as a percentage of control (no LPA) and represent the mean $\pm$ SEM ($n = 3$–4). *, $P < 0.05$ vs. no LPA (using Student's *t* test). (*B*) Effect of LPA on [^{35}S]-GTPγS binding to membranes of control and experimental B103 stable cell lines and cortical neuroblast cell line TSM. Basal [^{35}S]-GTPγS binding was 45.7 $\pm$ 2.5 (B103), 61.9 $\pm$ 2.1 (E-7), 57.2 $\pm$ 4.2 (A-5), 72.6 $\pm$ 3.7 (S-3), 73.9 $\pm$ 5.5 (S-7), and 83.3 $\pm$ 5.8 (TSM) cpm/μg protein. Data are expressed as described in *A* ($n \geq 3$). *, $P < 0.05$ (using Student's *t* test) vs. no LPA. (*C*) Effect of PTX treatment on LPA-induced [^{35}S]-GTPγS binding in clone S-3. Cells were treated without or with PTX. Basal [^{35}S]-GTPγS binding was 72.6 $\pm$ 3.4 (no PTX) and 71.1 $\pm$ 1.3 (PTX) cpm/μg protein. (*Inset*) Autoradiogram of PTX-catalyzed [^{32}P]-ADP ribosylation in membranes of S-3 cells pretreated without (*Left*) or with PTX (*Right*) demonstrates PTX functionality. Data are expressed as described in *A* ($n = 3$). *, $P < 0.05$ (using Student's

*t*test) vs. no LPA. #, $P < 0.05$ vs. no PTX. (*D*) Effect of structurally related phospholipids on [^{35}S]-GTPγS binding in clone S-3. Basal [^{35}S]-GTPγS binding was 91.9 $\pm$ 20.2 cpm/μg protein. Data are expressed as described in *A* ($n = 3$). *, $P < 0.05$ (using Student's *t* test) vs. no LPA. (E) VZG-1 couples to G_i after LPA stimulation. A-5 or S-3 cell membranes were labeled with [^{35}S]-GTPγS, and $G_{\alpha i}$ protein was immunoprecipitated as described in *Experimental Procedures*. Basal binding in the immunoprecipitates was 15.2 $\pm$ 4.7 (A-5) or 20.0 $\pm$ 6.9 cpm/μg protein (S-3). Data are expressed as described in *A* ($n = 3$). *, $P < 0.05$ (using Student's *t* test) vs. no LPA. (*F*) Western blot demonstrates expression of G proteins thought to mediate LPA signaling in mouse brain, B103, and RH7777 cell lines. Isolated membranes (50 μg) were subjected to Western blotting, as described (13). See Table 1 and *Experimental Procedures* for abbreviations.

were transfected transiently with the control (pflag), the pattern of actin-staining with TRITC–phalloidin was diffuse throughout cells as seen with untransfected cells (Fig. 3*A*) and was unaffected by LPA exposure (Fig. 3*B*). By contrast, cells transfected with pflag/vzg-1 were immunostained specifically by anti-flag antibody (Fig. 3*C*), and phalloidin labeling in these cells was always more intense than that in untransfected cells (Fig. 3*D*). Indeed, a small percentage of VZG-1-expressing cells showed stress fibers in the absence of LPA. However, when 100 nM LPA was added to cultures of VZG-1-expressing cells, dramatic stress fibers were observed in flag-positive cells (Fig. 3 *E* and *F*). Stress fiber formation after LPA exposure was dose-dependent (EC$_{50}$ = 4 nM; Fig. 3*G*). Similar results were obtained by using another expression vector, pHook2/vzg-1 (data not shown, but see Fig. 5), indicating that LPA-dependent responses were not caused by the expression vector *per se*. To determine whether LPA-stimulated VZG-1 activates stress fiber formation through Rho, C3 exoenzyme, which ADP ribosylates and inactivates Rho, was used (11, 15, 27, 28). When RH7777 cells expressing VZG-1 were preincubated with functional recombinant his-C3 exoenzyme and stained with TRITC-labeled phalloidin, stress fiber formation was limited to control levels and was unaffected by LPA stimulation (Fig. 3*G*). Stress fiber formation by LPA was not reproduced by other lysophosphatidic compounds or phosphatidate (Fig. 3*H*), consistent with previous data (13). Thus, activated Rho

is involved in VZG-1-dependent stress fiber formation after LPA stimulation.

Neurite Retraction Is Dependent on VZG-1 Expression and LPA Stimulation and Also Is Mediated by Rho. Contrasting with cells from mesenchymal lineage such as fibroblasts, cells of neuronal lineage that respond with cytoskeletal changes to LPA do not form stress fibers but rather change their morphology by retracting neurites and producing a cell of spherical appearance ("cell rounding"; refs. 11 and 13). The majority of control B103 cells (as well as sense S-3 and antisense A-5) have long processes when grown under serum-free conditions (Fig. 4 *A*, *C*, and *E*). This morphology remained unchanged after control B103 or A-5 cells were exposed to LPA (up to 1 μM; Fig. 4 *B* and *D*). In sharp contrast, S-3 cells retracted neurites after LPA exposure (Fig. 4*G*), accompanied by actin rearrangement, based on staining with TRITC–phalloidin (data not shown). The same response to LPA was observed with two other independent sense clones, S-4 and S-7, and the effect was dose-dependent (1 nM–1 μM; Fig. 4*G*); the EC$_{50}$ was 4, 4, and 2 nM for S-3, S-4, and S-7, respectively. His-C3 exoenzyme but not PTX prevented the retraction of neurites by LPA, indicating that VZG-1 mediates neurite retraction by LPA through activated Rho in cells of neuronal lineage (Fig. 4H).

SRE Activation and DNA Synthesis Are Enhanced by VZG-1 Expression and LPA Stimulation. SRE is a regulatory region found in many growth factor-regulated promoters, and LPA has
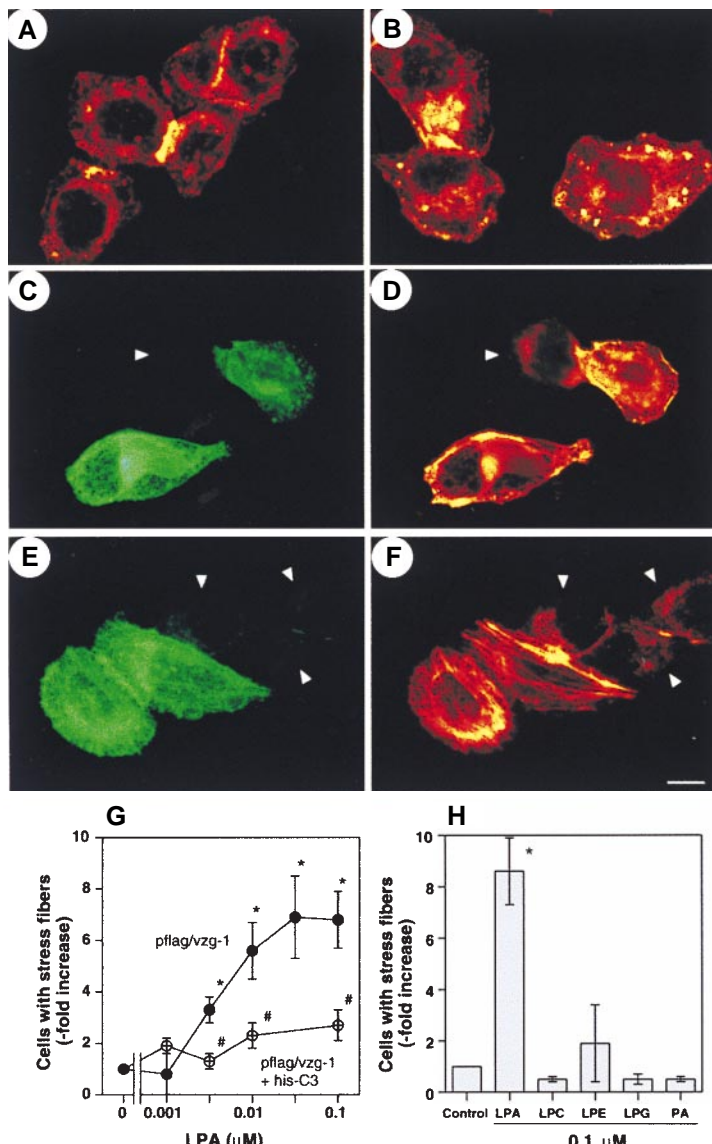

Fig. 3. VZG-1 mediates stress fiber formation by LPA in RH7777 cells through Rho activation. Immunofluorescent microscopy of RH7777 cells transfected with pflag (*A* and *B*) or pflag/vzg-1 (*C* to *E*) and then exposed to LPA at 0 nM (*A*, *C*, and *D*) or 100 nM (*B*, *E*, and *F*) for 15 min. Cells were fixed and double-labeled for flag-epitope (using M2 antibody visualized by indirect immunofluorescence using fluorescein isothiocyanate; *C* and *E*) and actin (visualized with TRITC-phalloidin; *A*, *B*, *D*, and *F*). Note that stress fibers are observed only with VZG-1 expression and LPA exposure (*E* and *F*). Arrowheads, nontransfected cells. (Bar = 10 μm.) (*G*) Effect of his-C3 exoenzyme on LPA-induced stress fiber formation in VZG-1-expressing cells. RH7777 cells transfected with pflag/vzg-1 were treated without or with his-C3 exoenzyme, exposed to varying concentrations of LPA, and double-labeled for flag epitope and actin. The change in the number of double-labeled cells with stress fibers after LPA exposure compared with control (no LPA) was expressed as "fold increase." Data are the mean ± SEM (*n* = 4). ∗, *P* < 0.05 (using Student's *t* test) vs. no LPA. #, *P* < 0.05 vs. no C3 exoenzyme. (*H*) Effect of structurally related phospholipids on VZG-1-mediated stress fiber formation in pflag/vzg-1-transfected RH7777 cells. Data are the mean ± SEM (*n* = 3). ∗, *P* < 0.05 (using Student's *t* test) vs. no LPA. See *Experimental Procedures* for abbreviations.
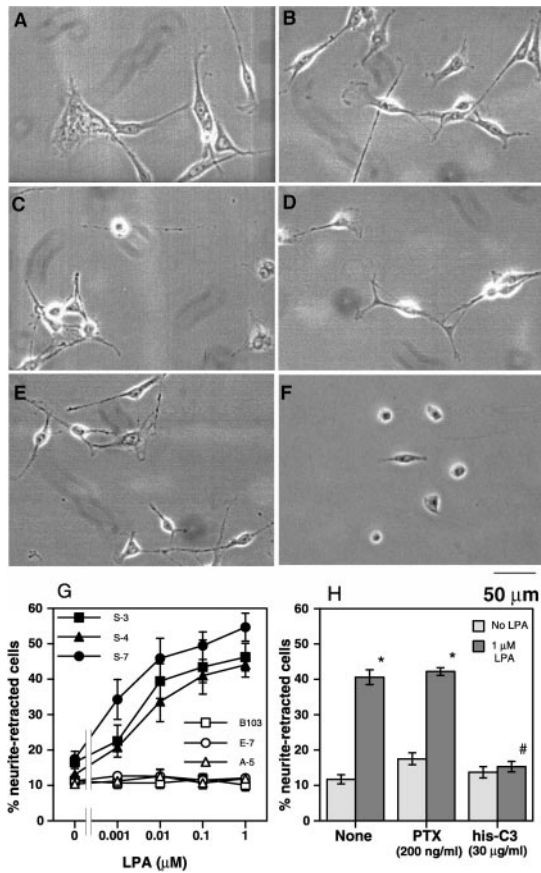
FIG. 4.   VZG-1 is required for LPA-dependent neurite retraction/cell rounding through Rho activation. Phase contrast microscopy of parental B103 cells (*A* and *B*), stable clone for antisense *vzg-1* (clone A-5; *C* and *D*) or a stable clone for sense *vzg-1* (clone S-3; *E* and *F*). Cells were treated with control vehicle buffer (*A, C,* and *E*) or with 1 μM LPA (*B, D,* and *F*) for 30 min. Only the sense-transfected cells exposed to LPA retracted neurites (*F*). (*G*) Dose–response relationship of LPA to neurite retraction in control and experimental B103 stable cell lines. Three independently derived, sense-expressing cell lines (S-3, S-4, and S-7) were compared with control cell lines (B103, parental line; E-7, empty vector-transfected line; and A-5, antisense-transfected line). Cells were treated with varying concentrations of LPA and fixed, and the percentages of neurite-retracted cells were determined. Data are the mean ± SEM ($n \geq 3$). Only *vzg-1* sense-transfected lines respond to LPA exposure. (*H*) Effect of functional PTX or his-C3 exoenzyme on LPA-induced neurite retraction. Sense-expressing clone S-3 was incubated with or without PTX or his-C3 exoenzyme and then analyzed for neurite retraction/cell rounding. Data are the mean ± SEM ($n = 4$). ∗, $P < 0.05$ (using Student's *t* test) vs. no LPA. #, $P < 0.05$ vs. 1 μM LPA in nontreated cultures (None). See *Experimental Procedures* for abbreviations.

been shown to activate the c-*fos* SRE (3, 4). To investigate whether VZG-1 can mediate LPA stimulation of SREs, B103 cells stably expressing CAT under c-*fos* SRE regulation (cell line C-1) were used to examine the effects of VZG-1 expression. LPA increased CAT protein expression only in pHook2/vzg-1-transfected cells in a dose-dependent manner (Fig. 5*A*). SRE activation by VZG-1 expression and LPA exposure was blocked completely by either pretreatment with PTX or his-C3 exoenzyme (Fig. 5*A*). Mitogenic effects of LPA, determined by BrdU incorporation, were observed in a *vzg-1* sense clone, S-3 (Fig. 5*B*) but not in control B103 nor A-5 (data not shown). The increase in BrdU incorporation by LPA was blocked completely by pretreatment of cells with PTX (Fig. 5*B*). In addition, his-C3 exoenzyme partially inhibited these LPA effects (Fig. 5*B*). These data indicate that VZG-1 is a receptor for LPA that mediates

both SRE activation and a subsequent event, cell cycle progression, through the G_i/G_o and Rho pathways.

DISCUSSION

A wide range of biological activities in a variety of neural and nonneural cell types has been documented for LPA (6). However, whether these activities were mediated by a single LPA receptor, several distinct receptors, or nonreceptor mechanisms has been unclear. In this study, we have made use of heterologous expression of VZG-1, a functional mammalian LPA receptor (13). Heterologous VZG-1 expression mediates at least six previously reported biological responses to LPA, including the production of [³H]-LPA membrane binding sites, LPA-dependent G protein activation, stress fiber formation, neurite retraction, transcriptional SRE activation, and increased DNA synthesis. These data
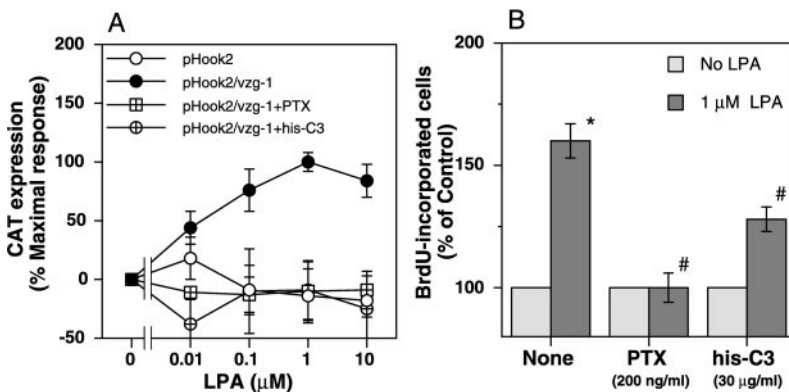

FIG. 5.   VZG-1 expression and LPA exposure activate SREs and increase DNA synthesis through both PTX- and C3-sensitive signaling pathways. (*A*) Effect of PTX or his-C3 exoenzyme on SRE activation by LPA through VZG-1 expression. Stable B103 cells containing CAT driven by *c-fos* SREs (clone C-1) were transfected transiently with pHook2 or pHook2/vzg-1, treated without or with PTX or his-C3 exoenzyme, and treated with varying LPA concentrations, and SRE activation determined. Basal CAT expression was 229 ± 36 (pHook2) or 191 ± 20 pg/mg protein (pHook2/vzg-1). Data are expressed as a percentage of maximal response at 1 μM LPA over control (no LPA), the mean ± SEM ($n \geq 4$). LPA at 0.1–10 μM significantly increased CAT expression in pHook2/vzg-1-transfected cells ($P < 0.05$ vs. no LPA using Student's *t* test). Both PTX and his-C3 exoenzyme significantly blocked LPA-induced increase in CAT ex-pression ($P < 0.05$ vs. no treatment with toxins). (*B*) Effect of PTX or his-C3 exoenzyme on DNA synthesis stimulated by LPA through VZG-1 expression. The S-3 cells were treated without or with PTX or his-C3 exoenzyme and DNA synthesis assayed after 24 h by a 1-h BrdU pulse. Basal percentages of BrdU-incorporated cells were 19.6 ± 1.9 (no treatment), 22.7 ± 2.0 (PTX), or 24.8 ± 1.6% (his-C3). Data are expressed as a percentage of control (no LPA), mean ± SEM ($n = 3–6$). ∗, $P < 0.05$ vs. no LPA. #, $P < 0.05$ (using Student's *t* test) vs. 1 μM LPA in nontreated culture.

demonstrate that a single G protein-coupled receptor, VZG-1, is necessary and sufficient for mediating multiple effects produced by LPA stimulation. It signals through at least two distinct pathways—a G_i/G_o pathway and a PTX-insensitive pathway that involves Rho activation—in *vzg-1* null cell lines from both a neuronal and nonneuronal lineage (Fig. 6).

LPA has been implicated in the activation of several G proteins that have been defined by their sensitivity—or lack of sensitivity—to PTX (1, 7, 10, 29–31). The PTX-sensitive response has indicated the involvement of G_i and/or G_o, activation of the former producing inhibition of adenylyl cyclase (1, 10, 31). We have shown previously that VZG-1 mediates inhibition of adenylyl cyclase by LPA in cortical neuroblast cell lines (13). Present data from the $[^{35}S]$-GTPγS labeling (Fig. 2 *C* and *E*) demonstrate that, indeed, G_i couples directly with VZG-1 after LPA exposure. At the same time, VZG-1 also mediates actin-based cytoskeletal changes that operate through a PTX-insensitive, but Rho-sensitive, pathway, but does so with phenotypically different results depending on the lineage of the cells examined (stress fiber formation in nonneuronal cells vs. neurite retraction and cell rounding in neuronal cell lines). The mechanisms responsible for this difference must be downstream of Rho activation in view of the effects of C3 exoenzyme.

Activation of SRE-dependent transcription is regulated by several proteins, including serum response factor and ternary complex factor (32). Stimulation of Ras–Raf–mitogen-activated protein kinase cascade links to SRE activation through ternary complex factor (33), and Rho mediates SRE activation through signaling to serum response factor (4). Our data indicate that VZG-1 activation by LPA increases transcription through exogenous SREs via both G_i/G_o and Rho pathways, based on decreased reporter gene expression by either functional PTX or C3 exoenzyme. This result is consistent with data showing that LPA-induced *c-fos* transcription is mediated by both Rho (4) as well as G_{i2} (5). Thus, VZG-1 transduces LPA signals into the same DNA target through two separate pathways. This overlap may reflect differences in the levels of upstream pathway activation and/or downstream gene transcription that result in a spectrum of cellular responses.

One important response that can be related to SRE activation is progression of the cell cycle. Indeed, VZG-1 also mediated mitogenic effects of LPA, which are blocked by either PTX or C3 exoenzyme, similar to SRE activation. These data are consistent further with the dual-pathway stimulation of SREs noted above and the roles of both G_i (1, 10, 34), and Rho (12, 15, 35) in stimulating DNA synthesis and cell growth.

From the presented data and independent studies with mammalian cells (36) and yeast (37), a single LPA receptor, VZG-1/LPA$_{A1}$/EDG-2, is capable of mediating multiple cellular responses by LPA in both neuronal and nonneuronal cells to regulate cell morphology and growth. Such multifunctional potential, for cells from different lineages, suggests biological consequences that, in the absence of specific LPA antagonists, may be discernible through molecular genetic approaches. In addition, the use of similar heterologous expression approaches should be useful in determining the role of nonreceptor mechanisms and receptor mechanisms mediated by other related receptors. As the first identified member of a growing family of homologous lysophospholipid receptor genes (J.C., J.J.A.C., and D.M., unpublished work), *vzg-1* provides an archetypal model for how receptors for other lipids, including sphingosine-1-phosphate and lysosphingomyelin, mediate cell signaling (38).

Note Added in Proof. Please see ref. 39 for review and discussion of receptor genes and nomenclature.

1. van Corven, E. J., Groenink, A., Jalink, K., Eichholtz, T. & Moolenaar, W. H. (1989) *Cell* **59**, 45–54.
2. Ridley, A. J. & Hall, A. (1992) *Cell* **70**, 389–399.
3. Hill, C. S. & Treisman, R. (1995) *EMBO J.* **14**, 5037–5047.
4. Hill, C. S., Wynne, J. & Treisman, R. (1995) *Cell* **81**, 1159–1170.
5. Chuprun, J. K., Raymond, J. R. & Blackshear, P. J. (1997) *J. Biol. Chem.* **272**, 773–781.
6. Moolenaar, W. H., Kranenburg, O., Postma, F. R. & Zondag, G. C. (1997) *Curr. Opin. Cell Biol.* **9**, 168–173.
7. Seewald, S., Sachinidis, A., Düsing, R., Ko, Y., Seul, C., Epping, P. & Vetter, H. (1997) *Atherosclerosis* **130**, 121–131.
8. Howe, L. R. & Marshall, C. J. (1993) *J. Biol. Chem.* **268**, 20717–20720.
9. Kumagai, N., Morii, N., Fujisawa, K., Yoshimasa, T., Nakao, K. & Narumiya, S. (1993) *FEBS Lett.* **329**, 273–276.
10. van Corven, E. J., Hordijk, P. L., Medema, R. H., Bos, J. L. & Moolenaar, W. H. (1993) *Proc. Natl. Acad. Sci. USA* **90**, 1257–1261.
11. Jalink, K., van Corven, E. J., Hengeveld, T., Morii, N., Narumiya, S. & Moolenaar, W. H. (1994) *J. Cell Biol.* **126**, 801–810.
12. Olson, M., Ashworth, A. & Hall, A. (1995) *Science* **269**, 1270–1272.
13. Hecht, J. H., Weiner, J. A., Post, S. R. & Chun, J. (1996) *J. Cell Biol.* **135**, 1071–1083.
14. Guo, Z., Liliom, K., Fischer, D. J., Bathurst, I. C., Tomei, L. D., Kiefer, M. C. & Tigyi, G. (1996) *Proc. Natl. Acad. Sci. USA* **93**, 14367–14372.
15. Yamamoto, M., Marui, N., Sakai, T. M., N, Kozaki, S., Ikai, K., Imamura, S. & Narumiya, S. (1993) *Oncogene* **8**, 1449–1455.
16. Thomson, F. J., Perkins, L., Ahern, D. & Clark, M. (1994) *Mol. Pharmacol.* **45**, 718–723.
17. Becker, J. E., de Nechaud, B. & Potter, V. R. (1976) in *Two New Rat Hepatoma Cell Lines for Studying the Unbalanced Blocked Ontogeny Hypothesis*, eds. Fishman, W. H. & Sell, S. (Academic, New York), pp. 259–270.
18. Schubert, D., Heinemann, S., Carlisle, W., Tarikas, H., Kimes, B., Patrick, J., Steingach, J. H., Culp, W. & Brandt, B. L. (1974) *Nature (London)* **249**, 224–227.
19. van der Bend, R. L., Brunner, J., Jalink, K., van Corven, E. J., Moolenaar, W. H. & van Blitterswijk, W. J. (1992) *EMBO J.* **11**, 2495–2501.
20. Lazareno, S. & Birdsall, N. (1993) *Br. J. Pharmacol.* **109**, 1120–1127.
21. Traynor, J. & Nahorski, S. (1995) *Mol. Pharmacol.* **47**, 848–854.
22. Selley, D., Sim, L., Xiao, R., Liu, Q. & Childers, S. (1997) *Mol. Pharmacol.* **51**, 87–96.
23. Williams, A., Michel, A., Feniuk, W. & Humphrey, P. (1997) *Mol. Pharmacol.* **51**, 1060–1069.
24. Chun, J. & Jaenisch, R. (1996) *Mol. Cell. Neurosci.* **7**, 304–321.
25. Hepler, J., Kozasa, T., Smrcka, A., Simon, M., Rhee, S., Sternweis, P. & Gilman, A. (1993) *J. Biol. Chem.* **268**, 14367–14375.
26. Singer, W., Miller, R. & Sternweis, P. (1994) *J. Biol. Chem.* **269**, 19796–19802.
27. Aktories, K., Braun, S., Rosener, S., Just, I. & Hall, A. (1989) *Biochem. Biophys. Res. Commun.* **158**, 209–213.
28. Paterson, H., Self, A., Garrett, M., Just, I., Aktories, K. & Hall, A. (1990) *J. Cell Biol.* **111**, 1001–1007.
29. Carr, C., Grassie, M. & Milligan, G. (1994) *Biochem. J.* **298**, 493–497.
30. Pietruck, F., Busch, S., Virchow, S., Brockmeyer, N. & Siffert, W. (1997) *Naunyn Schmiedebergs Arch Pharmacol.* **355**, 1–7.
31. Hordijk, P. L., Verlaan, I., van Corven, E. J. & Moolenaar, W. H. (1994) *J. Biol. Chem.* **269**, 645–651.
32. Hill, C. S., Wynne, J. & Treisman, R. (1994) *EMBO J.* **13**, 5421–5432.
33. Treisman, R. (1994) *Curr. Opin. Genet. Dev.* **4**, 96–101.
34. Inglese, J., Koch, W., Touhara, K. & Lefkowitz, R. (1995) *Trends Biochem. Sci.* **20**, 151–156.
35. Lamarche, N., Tapon, N., Stowers, L., Burbelo, P., Aspenstrom, P., Bridges, T., Chant, J. & Hall, A. (1996) *Cell* **87**, 519–529.
36. An, S., Dickens, M. A., Bleu, T., Hallmark, O. G. & Goetzl, E. J. (1997) *Biochem. Biophys. Res. Commun.* **231**, 619–622.
37. Erickson, J. R., Wu, J. J., Goddard, J. G., Tigyi, G., Kawanishi, K., Tomei, L. D. & Kiefer M. C. (1998) *J. Biol. Chem.* **273**, 1506–1510.
38. Meyer zu Heringdorf, D., van Koppen, C. J. & Jakobs, K. H. (1997) *FEBS Lett.* **410**, 34–38.
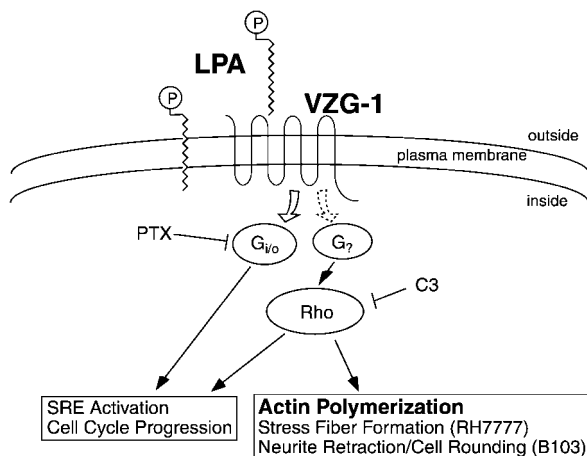39. Chun, J., Contos, J. J. A. & Munroe, D. (1998) *Cell Biochem. Biophys.*, in press.

FIG. 6.   VZG-1-Mediated responses after LPA stimulation, based on the presented heterologous expression studies.